Published in final edited form as:
J Neurosci Methods. 2012 July 15; 208(2): 190–196. doi:10.1016/j.jneumeth.2012.05.016.

Genetically-encoded fluorescent voltage sensors using the voltage-sensing domain of *Nematostella* and *Danio* phosphatases exhibit fast kinetics

Bradley J. Baker[1,2], **Lei Jin**[2], **Zhou Han**[2,3], **Lawrence B. Cohen**[1,2], **Marko Popovic**[2], **Jelena Platisa**[3,4], and **Vincent Pieribone**[2,3]

[1]Center for Functional Connectomics, Korea Institute of Science and Technology, Seoul 136-791, Republic of Korea

[2]Department of Cellular and Molecular of Physiology: Yale University School of Medicine, New Haven, CT, 06510, USA

[3]The John B. Pierce Laboratory, New Haven, CT 06519, USA

[4]Faculty of Physical Chemistry, University of Belgrade, Serbia

Abstract

A substantial increase in the speed of the optical response of genetically-encoded Fluorescent Protein voltage sensors (FP voltage sensors) was achieved by using the voltage-sensing phosphatase genes of *Nematostella vectensis* and *Danio rerio.* A potential *N. vectensis* voltage-sensing phosphatase was identified *in silico*. The voltage-sensing domain (S1–S4) of the *N. vectensis* homolog was used to create an FP voltage sensor called Nema. By replacing the phosphatase with a cerulean/citrine FRET pair, a new FP voltage sensor was synthesized with fast off kinetics (Tau_{off} <5 msec). However, the signal was small (ΔF/F= 0.6%/200 mV). FP voltage sensors using the *D. rerio* voltage-sensing phosphatase homolog, designated Zahra and Zahra 2, exhibited fast on and off kinetics within 2 msec of the time constants observed with the organic voltage-sensitive dye, di4-ANEPPS. Mutagenesis of the S4 region of the *Danio* FP voltage sensor shifted the voltage dependence to more negative potentials but did not noticeably affect the kinetics of the optical signal.

Keywords

genetically-encoded voltage-sensor; fluorescent protein; imaging membrane potential; voltage-sensing phosphatase

1. Introduction

The ability to image activity simultaneously from many locations enables the elucidation and characterization of neurons and circuits in response to stimuli (reviewed in Grinvald and Hildesheim, 2004; Knopfel et al., 2006). Over the past 40 years, organic dyes have been developed to measure biological variables such as calcium concentration, pH and membrane

potential (Brown et al., 1975; Davila et al., 1973; MacDonald and Jobsis, 1976). While extremely powerful in some circumstances, the nonspecific staining of all cell types is a significant drawback to elucidating the role of individual cell types involved in a neuronal circuit. It is usually impossible to discriminate the signals from a particular cell type from the summed signal from all cell types.

Genetically-encoded sensors could potentially alleviate this drawback since the expression of the sensor could be specified by the promoter used to drive transcription. In the past decade genetically-encoded calcium sensors have been developed for this purpose (Dreosti et al., 2009; Nakai et al., 2001; Tian et al., 2009). Genetically-encoded voltage sensors were first developed using the *Drosophila* Shaker channel with GFP positioned near the end of S6 (Siegel and Isacoff, 1997). This probe, FlaSh, was relatively slow with time constants of ~100 msec. Subsequently Ataka and Pieribone (2002) developed a fast sensor, SPARC, which had response time constants of <2msec. Unfortunately these early probes failed to produce significant membrane expression and usable signals in mammalian cells (Baker et al., 2007). More recent probes capable of reporting membrane potential changes in mammalian cells use the voltage-sensing, S1–S4, domain of the *Ciona intestinealis* voltage-gated phosphatase (Dimitrov et al., 2007; Murata et al., 2005; Tsutsui et al., 2008). These sensors are slow with rise time constants in tens of milliseconds and even slower declines of about 100 milliseconds.

A potential new member of the voltage-gated phosphatase gene family was identified in *N. vectensis* (sea anemone). Using this family member, a new FP voltage sensor was synthesized. This sensor exhibited a weaker but substantially faster optical signal in response to changes in membrane potential. To see if the voltage-gated phosphatase gene from other organisms would exhibit similar kinetics, the *D. rerio* voltage-sensing phosphatase homolog was used to generate new FP voltage sensors. These zebrafish-based sensors also exhibited fast optical signals with response time constants nearly as fast as the voltage-sensing dye, di4-ANEPPS. Mutations to ‘tune’ the voltage dependence of the optical signal yielded sensors that responded to more physiologically relevant voltage depolarizations without significantly altering the kinetics of the signal.

2. Materials and Methods

2.1 Sequence analysis

An expressed sequence tag from *Nematostella vectensis* (NCBI: XM_001639084.1) shows homology to the voltage-gated phosphatase of *Ciona* (Putnam et al., 2007). Using the phosphatase domain sequence as bait, a partial Expressed Sequence Tag from *Nematostella* was found via a blast search. Using the genomic database from the Department of Energy (http://www.jgi.doe.gov/) we were able to deduce a potential 5′ sequence for the *Nematostella* phosphatase gene. Sequence alignment of the voltage-gated phosphatase homologs was done with Clustal W (Larkin et al., 2007). Graphical representation of conserved residues was performed using the program, GeneDoc version 2.7.000 (Nicholas and Nicholas, 1997).

2.2 DNA plasmid designs and construction

A novel genetically-encoded FP voltage sensor, Nema, was designed using the putative *N. vectensis* voltage-sensing phosphatase sequence with the following characteristics. 1: The phosphatase domain was replaced with a cerulean/citrine FRET pair as described in Dimitrov et al. (2007). 2: The fusion site for the FRET pair is at nucleotide +705 downstream of the adenine of the start methionine codon. 3: At position +700 is the cleavage site for the Eco RV restriction enzyme to facilitate the swapping of the 5′ end with other homologous voltage-sensing phosphatase sequences. This Eco RV site can also be

used to change the FRET pair at the 3′ end of the voltage sensor. The codon usage of this sensor was then optimized for expression in mammalian cells. DNA synthesis was performed by GenScript. The sensor was subcloned into pcDNA3.1+hygromycin (Invitrogen) via a Hind III site.

A second genetically-encoded fluorescent voltage sensor was generated by replacing the 5′ *N. vectensis* sequence with the voltage-sensing domain of the *D. rerio* voltage-sensing phosphatase. IMAGE clone 7167382 was used as a template for the amplification of the 5′ voltage-sensing domain using the sense primer BB 373 (5′ATTAGCTAGCgccaccatggccACGTCTGTGCATTTTAACCCTGGGTTAGATTCC3′) and the reverse primer BB 359 (5′catgcgatatctTCTTTTGTTCTCTGAAACCATTCTCCTGGTG3′). An Eco RV/Nhe I double digest of the Nema/pcDNA3.1 construct removes the *N. vectensis* sequence and allows the fusion of the *Danio* PCR product to the FRET pair.

The Zebrafish FP voltage sensor mutant R153Q was created by a two step PCR process using the high fidelity polymerase Turbo Pfu (Stratagene). Sense primer BB 373 and reverse primer BB 375 (5′ GGAATGTCACCACCtgGGGAATCAGACTG3′) yielded a PCR product that contained the 5′ end of the sequence with the R153Q mutation. The 3′ segment of the sequence with the R153Q mutation was amplified using the sense primer BB 374 (5′CAGTCTGATTCCCcaGGTGGTGACATTCC3′) and the reverse primer BB 375. The entire sequence containing the R153Q mutation was then amplified in the second step using the two purified PCR products from the first step, the sense primer BB 373, and the reverse primer BB 359. A similar strategy was employed for all of the Zebrafish FP voltage sensor mutants. Mutant primers for Zebrafish T156R were the sense primer BB 376 (5′CTGATTCCCAGGGTGGTGAgATTCCTGAGGTCTC3′) and the reverse primer BB 377 (5′GAGACCTCAGGAATcTCACCACCCTGGGAATCAG3′). Zebrafish R153Q/T156R was generated using the mutant sense primer BB378 (5′CTGATTCCCcaGGTGGTGAgATTCCTGAGGTCTC3′) and the mutant reverse primer BB 379 (5′GAGACCTCAGGAATcTCACCACCtgGGGAATCAG3′). Zebrafish R153Q/I165R was generated using the mutant sense primer BB 380 (5′GAGGTCTCTGAGGATCCTAAggCTGGTACGC3′) and the mutant reverse primer BB 380 (5′GCGTACCAGccTTAGGATCCTCAGAGACCTC3′) and Zebrafish R153Q mutant as template. All constructs were verified by DNA sequencing.

2.3 Transient and stable expression of FP voltage sensors in mammalian cells

HEK 293 cells were plated onto poly-L-lysine coated coverslips. Transient transfections using lippofectamine 2000 (Invitrogen) were carried out following the manufacturer's instructions. Stable HEK 293 cell lines expressing Nema and the Zebrafish FP voltage sensors were generated by selection with DMEM high glucose (Sigma) supplemented with Fetal Bovine Serum (10% v/v) (Sigma) and hygromycin B at 200 ug/ml (Invitrogen). Non-transfected HEK cells showed zero viability after 7 days incubation in hygromycin B (100 ug/ml). At least five individual colonies were propagated in selection media for each construct.

2.4 Patch clamp and optical signal analysis

Coverslips with HEK 293 cells were kept at 30°C using a Warner instruments model SH-27B in-line heater and stage bath heater. Membrane potential was controlled by a Patch Clamp PC-505B amplifier (Warner Instruments). The pipette solution contained 120mM K-aspartate, 4mM NaCl, 4mM MgCl2, 1mM CaCl2, 10mM EGTA, 3mM Na2ATP and 5mM HEPES pH 7.2. The bath solution consisted of 150mM NaCl, 4mM KCl, 2mM CaCl2, 1mM MgCl2, 5mM d-glucose, and 5mM HEPES pH 7.4 as described in Baker et al, 2007(Baker

et al., 2007). We used the optical response of HEK293 cells stained with the organic voltage-sensitive dye, di4-ANEPPS, as an indicator of the speed of our single electrode voltage clamp. di4-ANEPPS had a very fast (<2 μsec) response time constant in measurements on squid axons where a very fast clamp can be obtained (Loew et al., 1985).

Arc lamp illumination—HEK 293 cells were imaged on a Nikon Eclipse E6000FN microscope (Nikon, Melville, NY) with a 60x, 1.0 N.A. water immersion lens using a 150W Xenon arc lamp (OptiQuip Highland Mills, NY). The filter cube in the microscope contains an excitation filter D420/30x(Chroma) and a dichroic mirror, 455DCLP (Chroma). The objective C-mount image was demagnified by an Optem zoom system A45699 (Qioptiq LINOS, Inc, Fairport, NY) and projected into an image splitter, Optosplit II (Cairn) which contains a second dichroic mirror Q515LP(Chroma) and two emission filters, D480/40M(Chroma) and HQ520LP(Chroma). The images of the two channels are projected onto the back-thinned e2v CCD39 chip of a NeuroCCD-SM 80 pixel × 80 pixel camera (RedShirtImaging, LLC, Decatur, GA). The imaging apparatus was mounted on a BM-1 Bench Top Vibration Isolation Platform (minus k Technology, Inglewood, CA). The mechanical shutter in the incident light path was mounted on a separate table and did not touch the microscope. A frame rate of 1 kfps was used for the optical recordings and 2 kHz for the electrode recordings. Sixty-four trials were averaged for each trace shown. Optical signal analysis was performed using NeuroPlex (RedShirtImaging). The traces are the spatial average of the output of all of the pixels receiving light from the cell. Taus were measured by calculating the time for the optical response to reach 0.63 of the maximal fluorescence change on unfiltered traces.

Laser illumination—Excitation light was from a 442nm laser (MLL-III-442 50mW; Changchun New Industries Optoelectronics Tech. Co., Ltd.). The laser was guided into the microscope by a multi-mode fiber coupler (Siskiyou), a quartz light-guide (Till Photonics) and an Achromatic EPI-Fluorescence Condenser (Till Photonics). The filter cube in the microscope contained a dichroic mirror 455DCLP (Chroma). The measured fluorescence is the average intensity of the pixels from the patched cell. 10 trials were averaged to improve the signal to noise ratio. Laser illumination was used for the experiments illustrated in Figures 5 and 6.

The off-line low-pass temporal filtering used to improve the signal-to-noise ratio is indicated in the figure legends.

Confocal microscopy was performed on a Zeiss LSM-510 META using a C-Apochromat 63x/1.2 water immersion objective.

3. Results

3.1 Potential voltage-sensing phosphatase homolog in *N. vectensis*

The expressed sequence tag, gene ascension number XM_001639084, was identified *in silica* using the phosphatase domain sequence of *Ciona intestinalis* voltage-sensing phosphatase as bait. Figure 1 shows the 5′ end of the EST which exhibits strong homology to the phosphatase domain and also has the positively charged arginine residues in the voltage-sensing, S4 transmembrane domain suggesting that this gene is also voltage-sensitive. To determine the 5′ end of the *Nematostella* voltage-sensing phosphatase gene, the genomic sequence was probed for upstream open reading frames using the Department of Energy Joint Genome Institute's web page (http://www.jgi.doe.gov). Open reading frames corresponding to the putative 5′ end of the *Nematostella* voltage-sensing phosphatase gene were found in reverse orientation on scaffold 16 from base pairs 222242-222165, 222071-221982, 220757-220719, 219948-219865, 219760-219530, and

219399-219301. As a guide to determine the 5′ end of the *Nematostella* voltage-sensing phosphatase gene, these open reading frames were aligned to other voltage-sensing phosphatase family members using the program Clustalw (http://www.ebi.ac.uk/Tools/clustalw/, (Larkin et al., 2007)). Potential exon/intron boundaries were identified using GENESCAN (Burge and Karlin, 1997). The final product is shown in supplemental figure 1.

3.2 Alignment of the *Nematostella* voltage-sensing phosphatase protein sequence with other voltage-sensing phosphatase homologs

The alignment illustrated in Figure 2 demonstrates high conservation of the phosphatase domain (PTEN) and significant conservation of the transmembrane domains, S1–S4. The positively charged arginines in transmembrane four (S4) are nearly invariable. The only exception is the lysine found in the S4 domain for *Nematostella* (figure 2). This lysine is actually an arginine in the EST sequence, but the genomic splice sites suggested the possibility of a lysine at this position. Whether the R1 position in *Nematostella* voltage-sensing phosphatase is an arginine or a lysine, the high conservation of the positive charges in S4 suggests that all of these homologs are responsive to voltage. The amino terminal, cytosolic region exhibited a high degree of variation in both length and protein composition (supplemental figure 2). To test whether the sequence variation of these homologs could improve the optical response of a fluorescent protein voltage sensor, the putative amino terminus sequence from the *Nematostella* voltage-sensing phosphatase was fused to the cerulean/citrine FRET pair used in the voltage sensor VSFP2.1 (Dimitrov et al., 2007). This construct, designated Nema, was synthesized allowing for the placement of restriction sites to facilitate the replacement of the fluorescent proteins or the voltage-sensing domain.

3.3 Nema exhibits an optical signal in response to membrane depolarizations

When expressed in HEK293 cells using whole-cell voltage clamp to control the membrane potential, Nema exhibits a small optical signal that could be seen when a very strong depolarization was used (Figure 3). Starting with a holding potential of −70 mV, an optical signal (0.4% Δ F/F in the YFP channel) can be seen with a 200 mV depolarization. The signal increases with even larger depolarizations. This need to strongly depolarize Nema is a characteristic shared among other members of the voltage-sensing phosphatase family (Dimitrov et al., 2007; Hossain et al., 2008; Murata et al., 2005). The voltage response can be ‘tuned’ by mutating the positive charges in the S4 domain, but the poor signal size discouraged further development of this probe.

While the size of the optical signal from Nema was disappointing the kinetics of the optical signal were significantly faster than those reported for VSFP 2.1 (Dimitrov et al., 2007; Lundby et al., 2008) or Mermaid (Tsutsui et al., 2008). The tau off was <5 ± 3msec. The tau on was 13 ± 6 msec. Both rates are substantially faster than VSFP 2.1 and Mermaid. This improvement in the kinetic responses encouraged the development of other FP voltage sensors. For this we tried the *Danio* voltage-sensing phosphatase homolog.

3.4 A *Danio* based FP voltage sensor had larger signals and faster kinetics

The original *Danio* based FP voltage sensor used the wildtype sequence designated Zebrafish WT. This sensor has the same design as Nema with the *Nematostella* sequence replaced by the corresponding *Danio* sequence. The Zebrafish WT FP voltage sensor exhibited a larger optical signal with faster on and off kinetics (Figure 4). Like Nema, the zebrafish WT FP voltage sensor required a depolarization of 200 mV in order to detect an optical signal (Figure 4). The signal size was better than Nema with a Δ F/F of about 6% in the CFP channel and 2% in the YFP channel for a 250 mV depolarization.

3.5 "Tuning" the voltage response of the Zebrafish WT FP voltage sensor to a physiologically relevant range

Mutations to the S4 domain of the zebrafish WT FP voltage sensor changed the voltage dependence of the optical signal. The impressive feature of the Zebrafish WT FP voltage sensor is its speed. To create optical signals for physiological voltage changes, mutations of the positive residues of the transmembrane, S4 domain were made. The voltage sensitivity of the *Danio* voltage-sensing phosphatase has been described (Hossain et al., 2008). Several mutations to the S4 were shown to shift the enzymatic response of the phosphatase to more negative membrane potentials. The same mutations were carried out on the zebrafish WT FP voltage sensor. The positively charged amino acids in the S4 domain occur every third amino acid. In the zebrafish WT FP voltage sensor the positively charged amino acids are arginines (R) with hydrophobic residues between (R_1-x-x-X_2-x-x-R_3-x-x-R_4). The numbered residues denote the position of positively charged amino acids in the S4 domain. Note that X_2 is actually a threonine unlike other voltage-gated proteins that normally have a positively charged residue at this position.

Mutagenesis of the R_1 position to the polar glutamine residue (R153Q) shifted the voltage dependence of the optical signal to more negative potentials. A very small signal can be seen with the 50 mV depolarization (Figure 4). A small but clear signal can be seen with the 100 mV depolarization. The R153Q mutation of the *Danio* voltage-sensing phosphatase showed a similar effect on the enzymatic activity (Hossain et al., 2008). The corresponding mutation in the *Ciona* voltage-sensing phosphatase and VSFP 2.1 (Dimitrov et al., 2007) also showed a similar voltage shift. This construct, the zebrafish FP voltage sensor with the R153Q mutation was designated Zahra.

Mutagenesis of the threonine in the R_2 position to arginine (T156R) also shifts the voltage response of the zebrafish WT FP voltage sensor to more negative potentials but not as much as R153Q (figure 4). This mutation creates the R_1-x-x-R_2-x-x-R_3-x-x-R_4 found in most voltage-gated channels. A clear optical signal can be seen with a 150 mV depolarization. The shift in the voltage response is not as large as that seen for Zahra since no optical signal can be detected for a 100 mV depolarization.

The double mutant R153Q/T156R does not have as much of an effect on the voltage-dependence as each individual mutation (figure 4). Only a small signal can be seen with a 150 mV depolarization compared to a larger signal at the 150 mV depolarization for the T156R mutant and a detectable signal for the R153Q mutant with a 50 mV depolarization.

The double mutant R153Q/I165R was shown to significantly shift the voltage dependence of *Danio* voltage-sensing phosphatase (Hossain et al., 2008). The Zebrafish R153Q/I165R FP voltage sensor, designated Zahra 2, also exhibited a strong shift in the voltage dependence of the optical response. A clear signal in the YFP channel could be seen with a 50 mV depolarization (Figure 4). The voltage-sensing domain of Zahra 2 may be shifted towards the carboxy-terminus since the mutant sequence results in Q_1-x-x-T_2-x-x-R_3-x-x-R_4-x-x-R_5-x-x-R_6. Figure 4 compares the optical signals at various membrane potentials of Zahra and Zahra 2 to the Zebrafish WT construct. All mutants failed to saturate even for a 250 mV depolarization suggesting that the maximum optical signal has not been reached. As a result plots of Δ F/F vs. voltage cannot be fit to a Boltzmann curve.

Zahra and Zahra 2 exhibited optical signals at physiologically relevant membrane potentials. All mutants described exhibited rather fast optical signals regardless of the size of the depolarization (Figure 4). The measured tau on for the YFP signal of Zahra 2 was 3.5 ±1.0 msec for a 100 mV depolarization while the corresponding tau off was 3.5 ± 1.7 msec (n=3,

error is standard deviation). The tuning of the S4 domain did not significantly alter the kinetics of the optical response.

3.6 Zahra 2 is nearly as fast as the organic voltage-sensitive dye, di4-ANEPPS

Using a 442 nm laser to improve the signal-to-noise ratio of the Zahra 2 signal again reveals a very fast sensor in the CFP signal (Figure 5). The laser illumination was 10x brighter than the arc-lamp light source. While the optical response to membrane depolarization is quick, the spectral physics underlying the fluorescent change is not entirely clear. Clearly there is a FRET component as the YFP fluorescence increases with a corresponding CFP fluorescent decrease. However, there are two temporal components in the YFP trace compared to only a single component in the CFP trace (n=3). There was also a much more rapid bleaching of the YFP signal (data not shown).

Earlier measurements made on a very fast time scale indicated that di4-ANEPPS responded to changes in membrane potential with a time constant of less than 2 μsec (Loew et al., 1985). We used optical measurements from this dye to compare the speed of our voltage clamp (Figure 6). The time course of the di4-ANEPPS signal in Figure 6 is likely to represent the real time course of the change in membrane potential of the voltage clamped HEK293 cell. The voltage clamp is the rate-limiting affect. Comparison of the on response of Zahra 2 to di4-ANEPPS demonstrates just how fast this sensor is. In Figure 5 the depolarization signal of the CFP of Zahra 2 was normalized and overlaid onto the depolarization signal from cells stained with di4-ANEPPS. The difference in timing between Zahra 2 and di4-ANEPPS at 0.63 of the fluorescence change was 1.3±0.4 msec for the depolarizations illustrated in Figure 6 (n=5, error is standard deviation). Even though the CFP signals are relatively noisy, it is clear that the Zahra 2 signal lags by ≤ 2 milliseconds behind the di4-ANEPPS signal. A similar analysis was done on the off signal with similar results (data not shown). Measurements on 2 other cells also reveal only a small difference between the Zahra 2 signal and that of di4-ANEPPS.

The observed tau of 1.3 ± 0.4 msec for the voltage sensing dye is in accordance with measurements reported (Blunck et al., 2004) and suggests that the whole-cell voltage clamp contributes to the time course of the optical response. The observed taus for Zahra 2 are, therefore, likely to be slower than the actual speed of the Zhara 2 signal.

4.0 Discussion

In order to resolve action potentials, a genetically-encoded FP voltage sensor needs to respond on a millisecond time scale. The voltage sensor SPARC based on the skeletal muscle sodium channel and eGFP (Ataka and Pieribone, 2002) showed rapid kinetics in *Xenopus* oocytes but failed to produce a signal in mammalian cells (Baker et al., 2007). The best mammalian FP voltage sensors to date utilizing the voltage-sensing domain of the *Ciona* voltage-sensing phosphatase have slow optical responses (Mutoh et al., 2011; Tsutsui et al., 2008). The discovery of the voltage-sensing phosphatase gene family (Kumanovics et al., 2002) provides many possibilities for finding residues that might significantly increase the speed of the optical signal. Here we show that FP voltage sensors that use the voltage-sensing domain from both the *Nematostella* and *Danio* voltage-sensing phosphatases have significantly faster on and off optical response time constants. Zahra and Zahra 2 rival the speed of di4-ANEPPS.

Mutations to the voltage-sensing domain of the *Danio* voltage-sensing phosphatase that shift the voltage response to more physiologically relevant potentials do not significantly alter the speed of the optical response suggesting that Zahra and Zahra 2 may be good *in vivo* sensors. Yet significant drawbacks remain. The signal of the *Danio*-based probes, Zahra and

Zahra 2, are not as large as the *Ciona* variants (Dimitrov et al., 2007; Perron et al., 2009) including Mermaid (Tsutsui et al., 2008). In addition the weak fluorescence in the CFP channel results in a noisy signal. Replacement of the CFP/YFP FRET pair with better FRET partners or single FPs could alleviate this problem. Indeed, changing the FP is a known parameter that can alter the optical response of genetically-encoded FP voltage sensors (Gautam et al., 2009; Guerrero et al., 2002; Perron et al., 2009). Voltage probes with response time constants of 1–2 msec are fast enough to faithfully monitor action potentials in cardiac tissue and in neurons of several animal models (e.g., Drosophila and Aplysia). On the other hand, probes of this speed would be less than ideal for monitoring mammalian action potentials at 37 °C because their slowness would reduce the signal size. Lastly, probes of this speed would not be adequate for monitoring the details of action potential propagation into axons, dendrites, and spines of mammalian neurons. These kind of questions are best studied with organic voltage sensitive dyes which are substantially faster (Holthoff et al., 2010).

An advantage of FP voltage sensors is the ability to manipulate the threshold at which the voltage-sensing domain responds. For example, an FP voltage sensor that would only respond at potentials near zero mV would then only detect action potentials. We and others have mutated the positive charges in the S4 transmembrane helix of the voltage-sensing domain to create FP voltage sensors that respond at membrane potentials near zero without significantly altering the speed of the optical signal. However, the signal size of Zahra and Zahra2 continue to increase with additional depolarizations which means that neuronal responses will only create a partial change in the fluorescent output. In contrast, some *Ciona*-based FP voltage sensors have a steeper fluorescence/voltage relationship and reach a maximal optical change around 0 mV (Dimitrov et al., 2007; Tsutsui et al., 2008). A neuronal response from a neuron expressing a *Ciona* based FP voltage sensor would then result in a maximum fluorescent change due to an action potential. One possible way to increase the speed of the *Ciona* FP voltage sensors is to incorporate *Danio* mutations in *Ciona*-based constructs. These efforts will generate a large repertoire of FP voltage sensors some of which could exhibit both fast kinetics and large optical signals.

Supplementary Material

Refer to Web version on PubMed Central for supplementary material.

Acknowledgments

This work was supported by the World Class Institute(WCI) Program of the National Research Foundation of Korea(NRF) funded by the Ministry of Education, Science and Technology of Korea (MEST) (NRF Grant Number: WCI 2009-003) The John B. Pierce Laboratory, Inc. and by NIH grants DC005259, U24NS057631, ARRA U24NS057631-03S1, and ARRA-R01NS065110.

5.0 References

Ataka K, Pieribone VA. A genetically targetable fluorescent probe of channel gating with rapid kinetics. Biophys J. 2002; 82:509–16. [PubMed: 11751337]

Baker BJ, Lee H, Pieribone VA, Cohen LB, Isacoff EY, Knopfel T, Kosmidis EK. Three fluorescent protein voltage sensors exhibit low plasma membrane expression in mammalian cells. J Neurosci Methods. 2007; 161:32–8. [PubMed: 17126911]

Blunck R, Starace DM, Correa AM, Bezanilla F. Detecting rearrangements of shaker and NaChBac in real-time with fluorescence spectroscopy in patch-clamped mammalian cells. Biophysical journal. 2004; 86:3966–80. [PubMed: 15189893]

Brown JE, Cohen LB, De Weer P, Pinto LH, Ross WN, Salzberg BM. Rapid changes in intracellular free calcium concentration. Detection by metallochromic indicator dyes in squid giant axon. Biophys J. 1975; 15:1155–60. [PubMed: 1201331]

Burge C, Karlin S. Prediction of complete gene structures in human genomic DNA. J of Mol Biol. 1997; 268:78–94. [PubMed: 9149143]

Davila HV, Salzberg BM, Cohen LB, Waggoner AS. A large change in axon fluorescence that provides a promising method for measuring membrane potential. Nat New Biol. 1973; 241:159–60. [PubMed: 4512623]

Dimitrov D, He Y, Mutoh H, Baker BJ, Cohen L, Akemann W, Knopfel T. Engineering and characterization of an enhanced fluorescent protein voltage sensor. PloS one. 2007; 2:e440. [PubMed: 17487283]

Dreosti E, Odermatt B, Dorostkar MM, Lagnado L. A genetically encoded reporter of synaptic activity in vivo. Nat Methods. 2009; 6:883–9. [PubMed: 19898484]

Gautam SG, Perron A, Mutoh H, Knopfel T. Exploration of fluorescent protein voltage probes based on circularly permuted fluorescent proteins. Front Neuroeng. 2009; 2:14. [PubMed: 19862342]

Grinvald A, Hildesheim R. VSDI: a new era in functional imaging of cortical dynamics. Nat Rev Neurosci. 2004; 5:874–85. [PubMed: 15496865]

Guerrero G, Siegel MS, Roska B, Loots E, Isacoff EY. Tuning FlaSh: redesign of the dynamics, voltage range, and color of the genetically encoded optical sensor of membrane potential. Biophys J. 2002; 83:3607–18. [PubMed: 12496128]

Holthoff K, Zecevic D, Konnerth A. Rapid time course of action potentials in spines and remote dendrites of mouse visual cortex neurons. The Journal of physiology. 2010; 588:1085–96. [PubMed: 20156851]

Hossain MI, Iwasaki H, Okochi Y, Chahine M, Higashijima S, Nagayama K, Okamura Y. Enzyme domain affects the movement of the voltage sensor in ascidian and zebrafish voltage-sensing phosphatases. The J Biol Chem. 2008; 283:18248–59.

Knopfel T, Diez-Garcia J, Akemann W. Optical probing of neuronal circuit dynamics: genetically encoded versus classical fluorescent sensors. Trends Neurosci. 2006; 29:160–6. [PubMed: 16443289]

Kumanovics A, Levin G, Blount P. Family ties of gated pores: evolution of the sensor module. The FASEB J. 2002; 16:1623–9.

Larkin MA, Blackshields G, Brown NP, Chenna R, McGettigan PA, McWilliam H, Valentin F, Wallace IM, Wilm A, Lopez R, Thompson JD, Gibson TJ, Higgins DG. Clustal W and Clustal X version 2.0. Bioinformatics. 2007; 23:2947–8. [PubMed: 17846036]

Loew LM, Cohen LB, Salzberg BM, Obaid AL, Bezanilla F. Charge-shift probes of membrane potential. Characterization of aminostyrylpyridinium dyes on the squid giant axon. Biophys J. 1985; 47:71–7. [PubMed: 3978192]

Lundby A, Mutoh H, Dimitrov D, Akemann W, Knopfel T. Engineering of a genetically encodable fluorescent voltage sensor exploiting fast Ci-VSP voltage-sensing movements. PloS one. 2008; 3:e2514. [PubMed: 18575613]

MacDonald VW, Jobsis FF. Spectrophotometric studies on the pH of frog skeletal muscle. PH change during and after contractile activity. J Gen Physiol. 1976; 68:179–95. [PubMed: 8583]

Murata Y, Iwasaki H, Sasaki M, Inaba K, Okamura Y. Phosphoinositide phosphatase activity coupled to an intrinsic voltage sensor. Nature. 2005; 435:1239–43. [PubMed: 15902207]

Mutoh H, Perron A, Akemann W, Iwamoto Y, Knopfel T. Optogenetic monitoring of membrane potentials. Exp Physiol. 2011; 96:13–8. [PubMed: 20851856]

Nakai J, Ohkura M, Imoto K. A high signal-to-noise Ca(2+) probe composed of a single green fluorescent protein. Nat Biotechnol. 2001; 19:137–41. [PubMed: 11175727]

Nicholas, KB.; Nicholas, HB, Jr. GeneDoc: a tool for editing and annotating multiple sequence alignments. 1997.

Perron A, Mutoh H, Akemann W, Gautam SG, Dimitrov D, Iwamoto Y, Knopfel T. Second and third generation voltage-sensitive fluorescent proteins for monitoring membrane potential. Front Mol Neurosci. 2009; 2:5. [PubMed: 19623246]

Siegel MS, Isacoff EY. A genetically encoded optical probe of membrane voltage. Neuron. 1997; 19:735–41. [PubMed: 9354320]

Tian L, Hires SA, Mao T, Huber D, Chiappe ME, Chalasani SH, Petreanu L, Akerboom J, McKinney SA, Schreiter ER, Bargmann CI, Jayaraman V, Svoboda K, Looger LL. Imaging neural activity in worms, flies and mice with improved GCaMP calcium indicators. Nat Methods. 2009; 6:875–81. [PubMed: 19898485]

Tsutsui H, Karasawa S, Okamura Y, Miyawaki A. Improving membrane voltage measurements using FRT with new fluorescent proteins. Nat Methods. 2008; 5:683–5. [PubMed: 18622396]

Highlights

A potential voltage-sensing phosphatase was identified in *Nematostella*

- Novel fluorescent protein voltage sensors were developed using the voltage-sensing domains from *Nematostella* and *Danio* voltage-sensing phosphatase homologs.
- The *Danio*-based fluorescent protein voltage sensors exhibit fast kinetics that are nearly as fast as the voltage-sensitive dye, di4-ANEPPS (<2msecs).

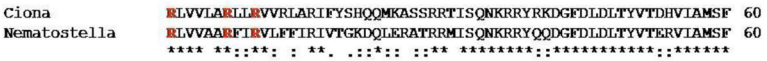

Figure 1.

Sequence alignment of Ciona VSP and Nematostella EST (gene accession number XM_001639084). The putative charged arginines of the S4 transmembrane domain are in red. The highly conserved SQNKRRY starts the PTEN phosphatase homology.

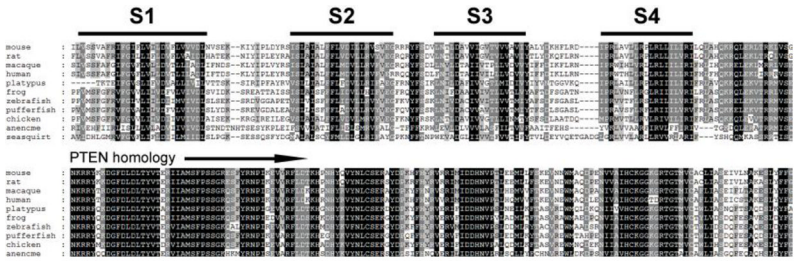

Figure 2.
Partial alignment of VSP family members. The putative S1 through S4 transmembrane domains are depicted. Conserved residues are shaded.

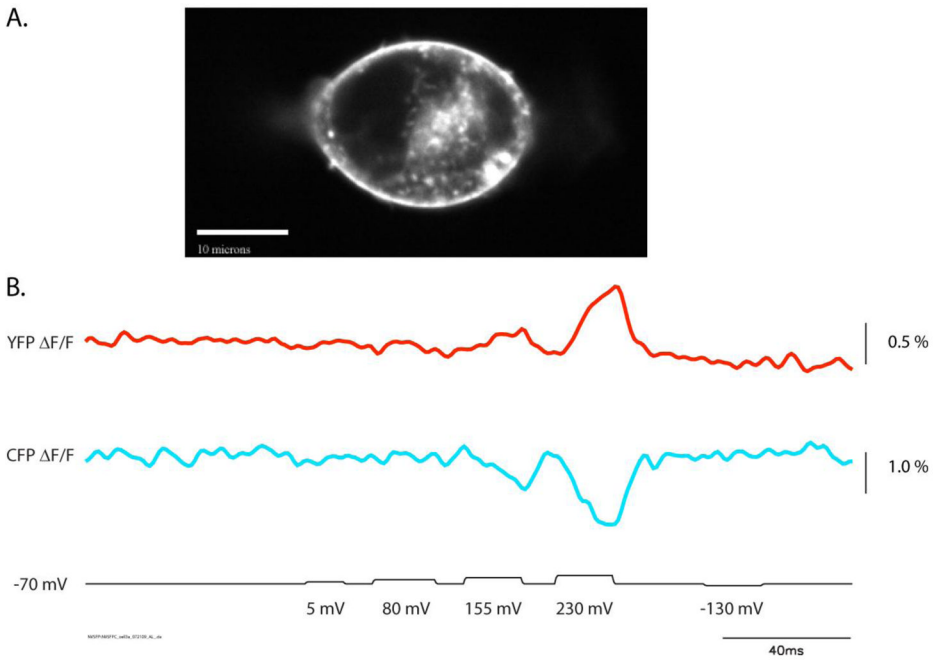

Figure 3.

A. Confocal z-stack image of an HEK-293 cell stably expressing the *N. vectensis* based FP voltage-sensor, Nema. B. Fluorescent trace of an HEK-293 cell expressing Nema. YFP fluorescence is in red. CFP fluorescence is in blue. Traces shown are the average of 64 trials. A low pass Gaussian filter of 100 Hz was used. Note the rapid off rate of the fluorescent signal.

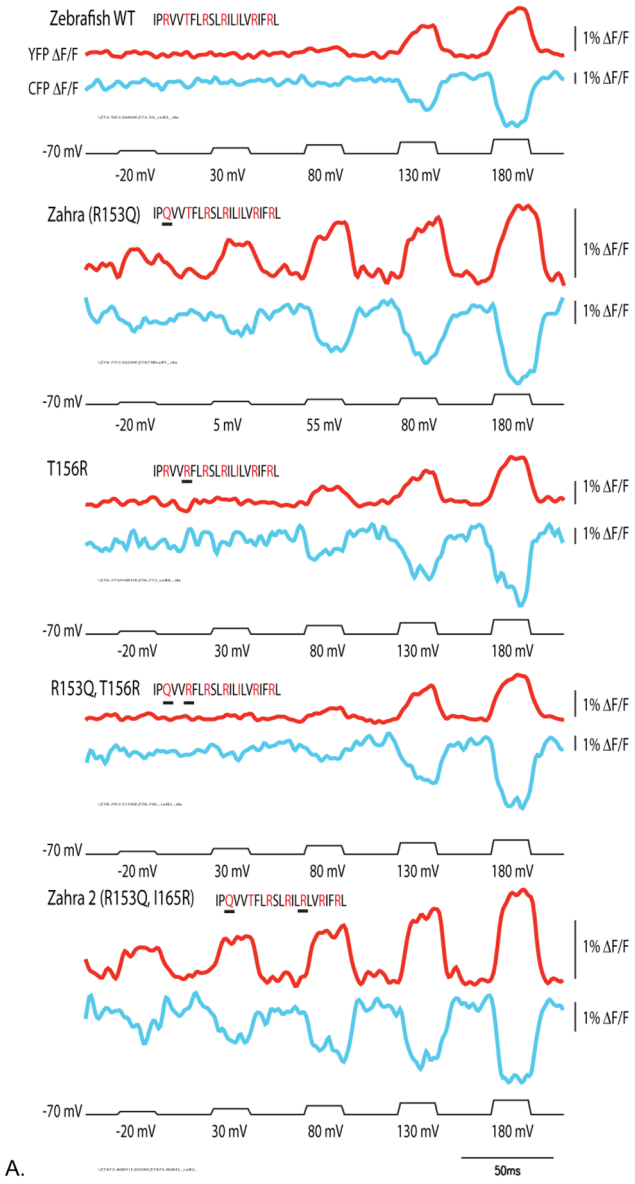

A.

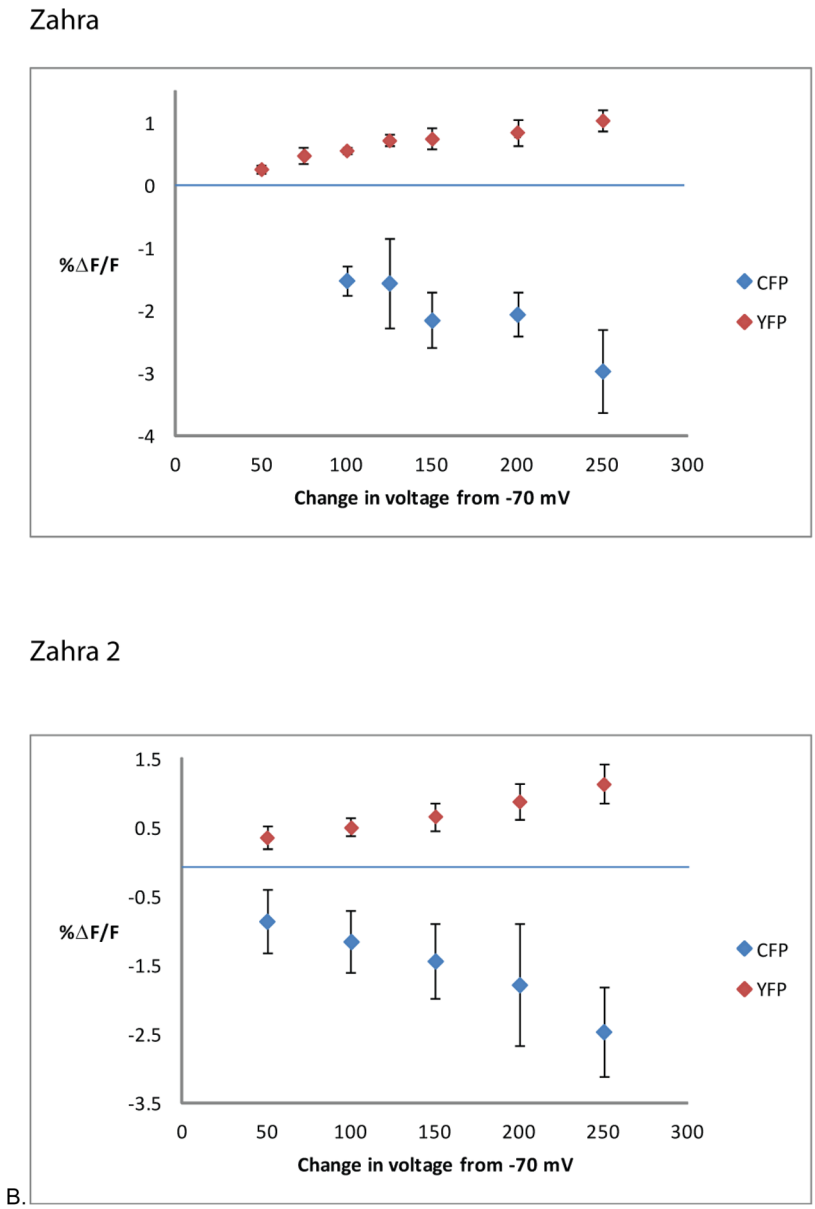

B.

Figure 4.

A. Mutation of the S4 domain results in two probes (Zahra and Zahra 2) that respond to physiological voltage changes. The Zebrafish WT probe with CFP (blue trace) and YFP (red trace) fluorescent changes in response to a series of voltage pulses (black trace). The protein sequence of the S4 domain is shown with residues in red representing the positively charged residues of the S4 α-helix. The point mutation that differs from the wildtype sequence is underlined. The T156R mutant and the R153Q/T156R double mutant did not shift the optical response as well as Zahra and Zahra2. A low pass Gaussian filter of 100 Hz was used for all traces. The traces are averages of 64 trials. B. Changes in fluorescence of Zhara and Zahra 2 were plotted versus membrane potential. A Boltzmann fit was not reliable since there was no observable maxima for any of the constructs tested. The CFP signal was not determined for the membrane depoloarizations to −20 mV and 5 mV due the noise of the CFP channel. The error bars are the standard deviations of 3 to 6 cells for each potential of Zahra and 4 cells for each potential of Zahra 2.

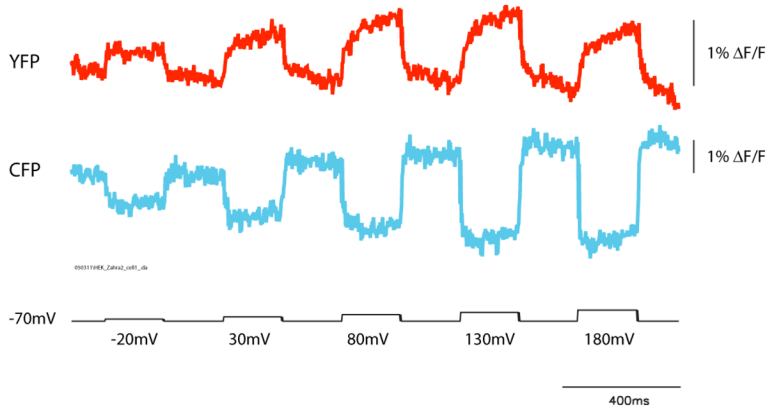

Figure 5.

ΔF/F Optical response of Zahra 2 to a sequence of five voltage steps using a 442 nm laser. HEK 293 cells expressing Zahra 2 were voltage-clamped and subjected to 200 msec depolarizations (black trace). The YFP fluorescence (red trace) and CFP fluorescence (blue trace) were filtered with a 100 Hz Gaussian low pass filter. YFP bleaching was compensated using a high pass filter. The traces are an average of ten trials.

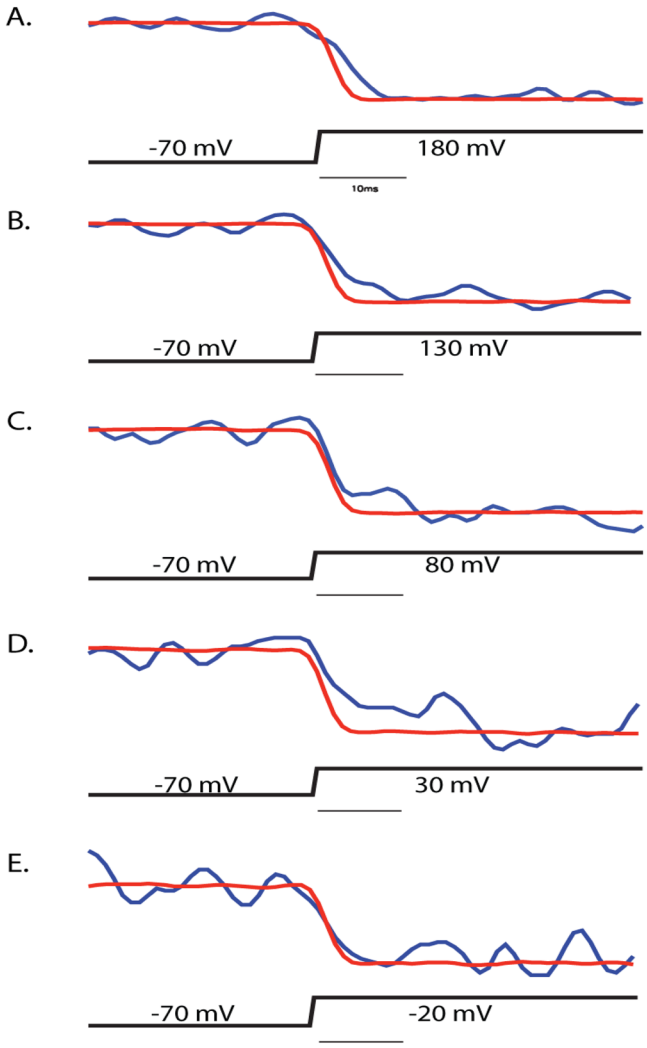

Figure 6.
Comparing the speed of Zahra 2 to di4-ANEPPS. The optical signal of Zahra 2 (blue trace) was normalized to the optical signal of HEK 293 cells stained with di4-ANEPPS (red trace). Cells were voltage-clamped at −70 mV and subjected to a 200 msec depolarization of: (A) 250 mV, (B) 200 mV, (C) 150 mV, (D), 100 mV, and (E) 50 mV.